Carbohydrate Research, 231 (1992) 171–183
Elsevier Science Publishers B.V., Amsterdam

The "pseudo double-helical" structure of the gel-forming capsular polysaccharide from *Rhizobium trifolii*

Eun J. Lee and Rengaswami Chandrasekaran

Whistler Center for Carbohydrate Research, Smith Hall, Purdue University, West Lafayette, Indiana 47907 (USA)

(Received October 4th, 1991; accepted January 29th, 1992)

ABSTRACT

X-ray diffraction analysis of oriented fibers of the gel-forming, neutral, doubly branched, galactose-rich capsular polysaccharide from *Rhizobium trifolii* has been used to determine and refine the molecular structure to a final R value of 0.28. The polysaccharide forms a 2-fold single helix of pitch 20.2 Å, is stabilized by a series of hydrogen bonds that involve the side chains, and has the appearance of a double helix. Packing calculations reveal that the short-range ordering of these "pseudo double helices" is brought about by intermolecular hydrogen bonds that involve the side chains. Complete or partial removal of side chains will weaken the molecular association and is detrimental to the gelation process.

INTRODUCTION

Water-soluble polysaccharides are used commonly as functional ingredients in the food industry in order to control the rheological properties which range from thickening (e.g., guaran and xanthan) to gelation (e.g., kappa-carrageenan and alginate) of the aqueous phase. When some functional requirements are not met by any of the established polysaccharides, new microbial polysaccharides are often sought. Before a new polysaccharide is approved for use in foods, it is necessary to determine its physical, chemical, and molecular properties in order to understand the structure–function relationships. As a part of a series of investigations of the structure of such gel-forming bacterial polysaccharides as gellan[1], kappa-carrageenan[2], and the gellan-related polysaccharides such as native gellan[3], welan, S-657, and rhamsan[4], we now report the three-dimensional structure of a galactose-rich polysaccharide from *Rhizobium*.

Correspondence to: Professor R. Chandrasekaran, Whistler Center for Carbohydrate Research, Smith Hall, Purdue University, West Lafayette, IN 47907, USA.

The doubly branched, hexasaccharide repeating unit **1** has been established[5,6] for the neutral, capsular polysaccharide (CPS) produced by *Rhizobium trifolii*, strain TA-1. Although double branching is a rare feature among bacterial polysaccharides, it is also present in some capsular polysaccharides from *Klebsiella*[7]. Because of the (1 → 6) linkage, the disaccharide side chain will have large conformational flexibility about its bond to the backbone. The polysaccharide is hot-water soluble and forms strong thermo-reversible gels that have melting/setting hysteresis at temperatures in the range 42–49° and in a wide range of concentrations (down to 0.2 mg/mL)[6,8]. Due to the non-ionic character of the polysaccharide chain, gels are formed in the absence of ionic co-solutes. The optical rotation and NMR spectra of the debranched polymer showed[6] that the elimination of side chains leads to loss of conformational ordering. In order to examine the role of the side chains on the gelling properties at the molecular level, the X-ray diffraction patterns were obtained from oriented fibers of the CPS, and stereochemically possible molecular models[9] were generated consistent with the observed helical parameters. The models include a 2-fold single helix, and a right- and left-handed, 4-fold, half-staggered, parallel, double helix[10]. The pitch of the double helix is twice that of the single helix. Without a detailed X-ray analysis, it was not possible then to adjudicate between the various helices. We now report the measurement of continuous X-ray intensities on layer lines and their use to refine each of the molecular models with the help of the linked-atom least-squares procedure[11]. The best model is a 2-fold single helix that has the appearance of an unconventional double helix. The details of the molecular structure are important for an understanding of gel formation.

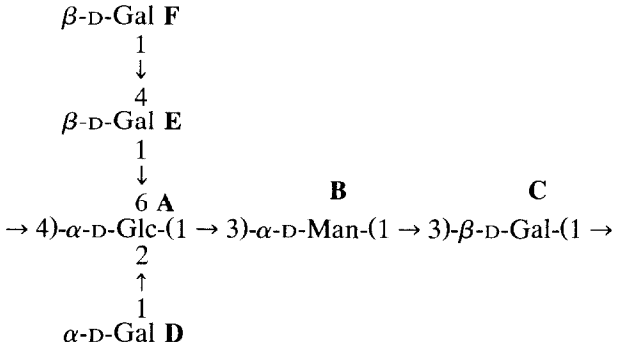

1

EXPERIMENTAL

X-ray intensity data.—Diffraction patterns were obtained from well-stretched and oriented fibers as described[9]. One of the best patterns is shown in Fig. 1. The distribution of intensities and lack of Bragg reflections suggest that the polysaccharide chains in the diffracting specimen are aligned reasonably along the fiber axis,

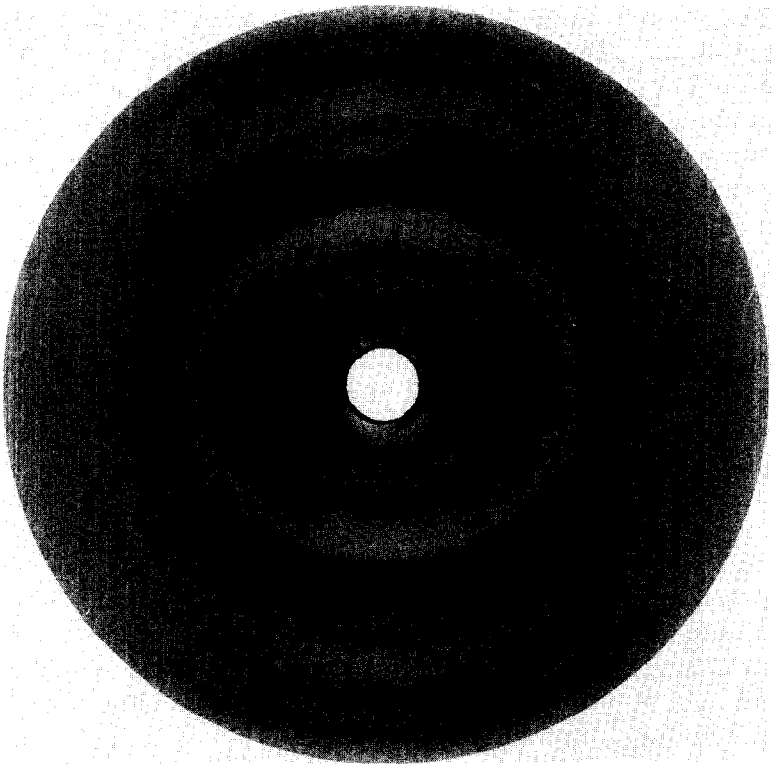

Fig. 1. X-ray diffraction pattern from a well-oriented fiber of the CPS. The intensities are almost continuously distributed on the layer lines. The strong meridional intensity on the second layer line indicates 2-fold helix symmetry.

and that their lateral organization is restricted to a short range. The film was calibrated internally by dusting the fiber with calcite powder and recording the ring of characteristic spacing 3.035 Å.

The diffraction pattern was digitized by using an Optronics P-1000 rotation drum microdensitometer with a 50-μm raster step. The digitized data were processed using a VAX 11/8558 computer and a Lexidata raster graphics system. The center and orientation of the diffraction pattern, fiber tilt to the X-ray beam, and c repeat were determined by standard methods[12]. A two-dimensional background function, expanded as a Fourier–Bessel series, was calculated from optical densities at positions between the layer lines and then subtracted from the original diffraction pattern[13]. The resulting continuous intensities were then sampled at intervals of 0.01 $Å^{-1}$ along every layer line, up to $\sim$3.5 Å resolution, then corrected for Lorentz and polarization effects[14].

The broad spot at a spacing of 16.8 Å and three other diffuse intensity maxima around 9.1, 6.0, and 3.6 Å on the equator and on higher layer lines, suggest some modest lateral organization. Using this information, it is possible to assign a

primitive monoclinic unit cell of dimensions $a = 16.8$ Å, $b = 9.7$ Å, $c = 20.2$ Å, and $\gamma = 90°$, or a trigonal cell with $a' = b' = 19.4$ Å, $c = 20.2$ Å, and $\gamma = 120°$. The relationship between the two cells is $a = a'\cos 30°$ and $b = a'/2$, so that the trigonal cell is twice as big as the monoclinic unit cell. The experimentally determined density of the fiber (1.47 g/mL) indicates that the small monoclinic cell can accommodate two (hexasaccharide) repeating units, each associated with ~ 28 water molecules. The large trigonal cell may contain twice this amount and therefore be relevant and useful, for example, for examining the packing arrangement of more than one chain in the unit cell[15].

Molecular-model building and analysis of the structure.—Polysaccharide helices of desired helical parameters were generated using standard geometries for the $^4C_1$ chair pyranose rings[16] for all six residues in the repeating unit. The bond angle at each glycosidic bridge oxygen atom was set initially at 116.5°. Hydrogen atoms were attached to the pyranose rings with appropriate stereochemistry. The 18 principal variables of the polysaccharide chain include the 6 sets of torsion angles (ϕ, ψ) at each disaccharide linkage, and the 6 rotations (χ) that define the orientations of the hydroxymethyl groups. In order to determine the range of sterically allowed torsion angles at each glycosidic linkage, hard-sphere maps were computed for each disaccharide moiety in **1**, including three maps for the (1 → 6) linkage, in disaccharide EA, corresponding to the three staggered domains with $\chi_1 = \sim 60°$, $\sim 180°$, and $\sim -60°$. Information on the allowed region served as important input for generating any helix model.

The first strong meridional-diffracted intensity (Fig. 1), present on the 2nd layer line (spacing 10.1 Å), implies that the polysaccharide forms a $2n$-fold helix. Consistent with the observed layer-line spacings, the main chain is either a 2-fold single helix of pitch 20.2 Å or a 4-fold, parallel, half-staggered, double helix of pitch 40.4 Å. The former helix is notionally achiral, but both right- and left-handed chiralities are to be considered for the latter. For each of these alternatives, the influence of all three staggered conformations about the (1 → 6) linkage on the overall helix geometry and on the X-ray fit was investigated, which accounts for a total of 9 different molecular models.

Each model was refined against the continuous X-ray data, so as to achieve a good fit with the experimental observations. Simultaneously, the steric compression within the molecule was optimized by minimizing the function Ω in a least-squares fashion[11] using the relationship

$$\Omega = \sum e_i({}_o\theta_i - \theta_i)^2 + \sum w_m({}_oT_m - T_m)^2 + \sum k_j({}_od_j - d_j)^2 + \sum \lambda_h G_h$$
$$= E + X + C + L$$

The first summation allows any refined conformation (or bond) angle θ_i to remain in its preferred domain ${}_o\theta_i$. The center of a disaccharide hard-sphere map, for example, corresponds to the preferred values for (ϕ, ψ). The second summation reduces the discrepancy between the observed (${}_oT_m$) and calculated (T_m) X-ray structure amplitudes. Hydrogen bonds, if any, are achieved and non-bonded short

contacts d_j are relieved towards higher values ${}_o d_j$ via the third summation. The quantities e_i, w_m, and k_j are the appropriate weights. The helix-connectivity constraints G_h become zero at the end of the analysis through the use of Lagrange multipliers λ_h. In the final stages of the refinement, the sugar rings were flexed by varying the 6 endocyclic conformation and 6 bond angles in each ring, subject to ring-closure constraints. The X-ray scale factor (K) was a variable during this joint X-ray contact refinement. One of the measures used to assess the correctness of a model was the conventional reliability index $R = \Sigma | {}_o T_m - T_m | / \Sigma_o T_m$. The statistics at the end of this analysis enabled a comparison of the relative merits of the different possibilities.

RESULTS

Single versus double helices.—The statistics of the 9 models generated with rigid sugars and refined against the X-ray data are listed in Table I. The single helix models (1–3), corresponding to χ_1 in the g^-, g^+, and t region, respectively, are stereochemically viable and model 1 has the lowest R value of 0.35 and also the lowest value for Ω. Among the double helices, $\chi_1 = g^-$ is rejected due to severe short contacts within the chain whether it is right- (model 4) or left-handed (model 7). In the other g^+ and t domains, models 5, 6, 8, and 9 are acceptable stereochemically. Application of Hamilton's significance test[17], based on X, C, Ω, or R, leads to the conclusion that the double helices are inferior to the single helices, and that, among the single helices, model 1 is superior to the rest at a 99.5% confidence level.

In further refining model 1, due to the absence of Bragg data, it was not possible to locate the water molecules associated with the polysaccharide chain. However, their contributions to the X-ray scattering were approximated by choos-

TABLE I

Statistics [a] for the single (1–3) and double helix (4–6 right-handed, 7–9 left-handed) models of the CPS

Model	χ_1	X	C	Ω	R
1	g^-	148	15	170	0.35
2	g^+	162	25	206	0.37
3	t	166	16	192	0.39
4	g^-		226		
5	g^+	236	20	266	0.44
6	t	167	18	196	0.37
7	g^-		162		
8	g^+	245	22	272	0.44
9	t	174	17	195	0.37

[a] X, C and Ω are, respectively, the X-ray, contact, and global terms in the function minimized by the least-squares procedure; R is the crystallographic reliability index. These values were not calculated for the stereochemically unacceptable models 4 and 7.

ing an appropriate solvent-electron density for the solvent-smeared atomic scattering factors. This approximation was done empirically by investigating the influence of varying the effective electron density of the solvent on the X-ray fit. By refining the X-ray-scale factor (K), R was surveyed at discrete values of σ, ranging from 0.8 to 1.8, where $\sigma = 1.0$ corresponds to the interstitial space filled with a continuum of water (electron density 0.2984 e/Å^3). The X-ray fit was far better ($R = 0.29$) at $\sigma = 1.4$ than at the other values examined. This finding suggests that the effective electron density of the solvent in the CPS fiber is ~ 1.4 times that of water alone. Final rounds of refinement with flexible sugar rings were conducted subsequently with $\sigma = 1.4$, which led to a small decrease in R to a value of 0.28. The atomic coordinates of the final 2-fold single helix (model 1) are given in Table II. The measured and calculated X-ray amplitudes are compared in Fig. 2. The agreement is very good, especially on the equator and 5th layer line, and acceptable for the remaining layer lines. The overall match is of the same kind as that reported for kappa-carrageenan, the molecular structure of which has been refined on the basis of continuous intensities[2].

Anatomy of the CPS helix.—The major conformational angles of model 1 are listed in Table III and they are all within the allowed regions. A side view of the molecule (Fig. 3) shows that the main chain follows a right-handed contour around the helix axis. The side chains are on the periphery across every glucose residue. The dispositions of the primary and secondary hydroxyl groups suggest that the stability of the molecule is derived from main chain–main chain, main chain–side chain, and side chain–side chain, interactions. The hydrogen bonds, some of them bifurcated, pertaining to one repeating unit are listed in Table IV. Within the main chain, the hydrogen bonds, O-3A · · · O-5C (cellulosic) and O-6B · · · O-2C, are noteworthy. Because of the sinuous nature of the helix, and since the conformation at the (1 → 6) linkage is g^-, the two terminal galactose residues, D and F (see **1**), are nearly equidistant from the helix axis and located in diametrically opposite positions. This arrangement facilitates the formation of side chain–side chain hydrogen bonds and the linking between adjacent repeating units. As a donor, O-4F forms bifurcated hydrogen bonds with O-2D and O-3D. Simultaneously, O-2D forms hydrogen bonds with O-3F. Thus, a series of side chain–side chain hydrogen bonds, involving the main-chain glucose residues, form a second discontinuous helix (DAEF) wrapped around the primary, inner main-chain helix (BAC). As a result, the CPS chain has the appearance of a double helix, and the figurative term "pseudo double helix" is suggested to denote this novel molecular architecture. The helix is further stabilized by hydrogen bonds within the disaccharide side chains (O-6E · · · O-5F and O-2F · · · O-3E) and between the main and side chains (O-3A · · · O-5D). The atom O-3A, as a donor, is located crucially (Fig. 3) to form bifurcated hydrogen bonds with the ring oxygen atoms O-5C and O-5D, which not only bind the monosaccharide side chain to the main chain but also facilitate interactions of the side chains. The 8 intrachain hydrogen bonds per hexasaccharide repeating unit described above stiffen the polysaccharide chain. The 3

TABLE II

Cartesian and cylindrical polar coordinates of the hexasaccharide repeating unit [a] of the 2-fold helix of CPS (See **1** for identities of A–F)

Unit	Atom	x(Å)	y(Å)	z(Å)	r(Å)	φ(°)	Unit	Atom	x(Å)	y(Å)	z(Å)	r(Å)	φ(°)
A	C-1	3.518	0.097	6.187	3.519	1.59	D	C-1	6.971	-0.160	7.189	6.973	-1.32
	C-2	4.621	0.291	7.219	4.630	3.60		C-2	7.881	-0.691	6.089	7.911	-5.01
	C-3	4.079	0.087	8.625	4.080	1.22		C-3	7.861	-2.211	6.068	8.166	-15.71
	C-4	2.858	0.967	8.856	3.017	18.70		C-4	8.178	-2.765	7.451	8.633	-18.68
	C-5	1.840	0.760	7.740	1.991	22.43		C-5	7.266	-2.127	8.493	7.571	-16.32
	C-6	0.655	1.695	7.849	1.817	68.88		C-6	7.619	-2.561	9.900	8.038	-18.58
	O-2	5.682	-0.618	6.950	5.715	-6.21		O-2	7.463	-0.162	4.836	7.464	-1.24
	O-3	5.091	0.408	9.581	5.108	4.58		O-3	8.823	-2.690	5.125	9.224	-16.96
	O-4	2.240	0.644	10.100	2.330	16.04		O-4	9.532	-2.485	7.799	9.851	-14.61
	O-5	2.448	1.004	6.462	2.646	22.30		O-5	7.385	-0.697	8.447	7.418	-5.39
	O-6	-0.349	1.180	8.721	1.230	106.50		O-6	7.391	-3.956	10.098	8.383	-28.16
	H-1	3.917	0.296	5.181	3.929	4.32		H-1	6.966	0.939	7.242	7.029	7.67
	H-2	5.033	1.307	7.129	5.200	14.56		H-2	8.909	-0.340	6.263	8.916	-2.18
	H-3	3.800	-0.969	8.761	3.921	-14.30		H-3	6.867	-2.560	5.753	7.328	-20.45
	H-4	3.180	2.019	8.869	3.767	32.42		H-4	8.032	-3.855	7.452	8.909	-25.64
	H-5	1.463	-0.273	7.775	1.488	-10.57		H-5	6.223	-2.415	8.293	6.675	-21.21
	H-61	0.224	1.859	6.850	1.872	83.13		H-61	8.675	-2.330	10.101	8.983	-15.03
	H-62	0.993	2.675	8.217	2.853	69.63		H-62	6.965	-2.045	10.618	7.259	-16.36
B	C-1	-0.058	-2.913	5.024	2.914	-91.14	E	C-1	-1.442	0.568	8.120	1.550	158.49
	C-2	0.922	-2.359	6.050	2.533	-68.65		C-2	-1.997	-0.476	9.080	2.053	-166.58
	C-3	2.043	-1.600	5.356	2.595	-38.08		C-3	-3.278	-1.080	8.525	3.451	-161.77
	C-4	2.701	-2.481	4.302	3.668	-42.57		C-4	-4.272	0.020	8.177	4.272	179.73
	C-5	1.643	-3.049	3.362	3.464	-61.68		C-5	-3.613	1.061	7.278	3.766	163.64
	C-6	2.217	-4.028	2.360	4.598	-61.17		C-6	-4.526	2.238	7.006	5.049	153.69
	O-2	1.443	-3.430	6.830	3.721	-67.19		O-2	-1.015	-1.484	9.296	1.798	-124.38
	O-3	3.013	-1.190	6.320	3.240	-21.55		O-3	-3.852	-1.959	9.494	4.322	-153.04
	O-4	3.635	-1.724	3.535	4.023	-25.38		O-4	-4.732	0.668	9.361	4.779	171.96
	O-5	0.642	-3.758	4.108	3.812	-80.31		O-5	-2.428	1.579	7.901	2.897	146.96
	O-6	1.255	-4.406	1.377	4.581	-74.10		O-6	-4.554	3.151	8.102	5.538	145.32
	H-1	-0.836	-3.496	5.539	3.594	-103.46		H-1	-1.137	0.139	7.155	1.146	173.05
	H-2	0.391	-1.685	6.738	1.730	-76.92		H-2	-2.202	-0.008	10.054	2.202	-179.79
	H-3	1.609	-0.713	4.871	1.760	-23.90		H-3	-3.048	-1.665	7.623	3.473	-151.35
	H-4	3.236	-3.305	4.795	4.626	-45.60		H-4	-5.137	-0.418	7.657	5.154	-175.35
	H-5	1.170	-2.228	2.603	2.517	-62.30		H-5	-3.348	0.599	6.316	3.401	169.86
	H-61	3.074	-3.567	1.846	4.709	-49.25		H-61	-4.187	2.763	6.100	5.016	146.58
	H-62	2.550	-4.937	2.884	5.556	-62.68		H-62	-5.544	1.874	6.805	5.852	161.32
C	C-1	-2.444	-1.527	1.052	2.882	-148.00	F	C-1	-6.108	0.739	9.537	6.152	173.10
	C-2	-1.312	-1.347	2.055	1.880	-134.26		C-2	-6.494	-0.186	10.684	6.496	-178.36
	C-3	-1.565	-2.164	3.313	2.670	-125.88		C-3	-7.971	-0.039	11.013	7.971	-179.72
	C-4	-2.950	-1.863	3.871	3.489	-147.73		C-4	-8.315	1.423	11.261	8.436	170.29
	C-5	-4.003	-2.025	2.781	4.486	-153.17		C-5	-7.830	2.282	10.098	8.156	163.75
	C-6	-5.385	-1.639	3.262	5.629	-163.07		C-6	-8.044	3.759	10.353	8.879	154.95
	O-2	-0.082	-1.728	1.449	1.730	-92.73		O-2	-6.186	-1.529	10.329	6.372	-166.11
	O-3	-0.575	-1.851	4.294	1.938	-107.25		O-3	-8.283	-0.811	12.175	8.322	-174.41
	O-4	-3.007	-0.526	4.364	3.053	-170.08		O-4	-7.692	1.884	12.458	7.920	166.24
	O-5	-3.687	-1.178	1.665	3.871	-162.28		O-5	-6.423	2.087	9.890	6.753	162.00
	O-6	-5.499	-0.233	3.476	5.504	-177.58		O-6	-6.991	4.320	11.136	8.218	148.29
	H-1	-2.478	-2.577	0.726	3.576	-133.88		H-1	-6.612	0.479	8.595	6.629	175.86
	H-2	-1.226	-0.284	2.323	1.259	-166.98		H-2	-5.894	0.061	11.572	5.894	179.41
	H-3	-1.497	-3.230	3.050	3.560	-114.87		H-3	-8.573	-0.420	10.175	8.583	-177.19
	H-4	-3.169	-2.553	4.699	4.070	-141.15		H-4	-9.405	1.531	11.367	9.529	170.75
	H-5	-4.032	-3.074	2.451	5.070	-142.67		H-5	-8.377	2.005	9.185	8.614	166.54
	H-61	-6.134	-1.960	2.523	6.440	-162.28		H-61	-8.110	4.291	9.392	9.175	152.12
	H-62	-5.610	-2.171	4.199	6.015	-158.84		H-62	-9.004	3.907	10.869	9.815	156.54

[a] Successive repeating units can be generated by applying 2-fold screw symmetry about the *z* axis.

intrachain hydrogen bonds between the mono- and di-saccharide side chains anchor and organize the side chains which, otherwise, will be conformationally flexible. These interactions are the main driving forces towards the adoption of an ordered conformation of the CPS molecule and the subsequent formation of ordered domains in the junction zones[18] involved in gel formation.

Molecular packing.—Although the X-ray data allowed the determination experimentally of only the molecular, but not the crystal, structure, the most probable packing arrangement of the CPS molecules in the monoclinic unit cell was modeled. This cell can accommodate only one 2-fold helix located at the origin, with its molecular axis coinciding with the *c* axis. Using the molecule as a rigid body, the only packing parameter is the orientation μ (rotation about the *c* axis) of

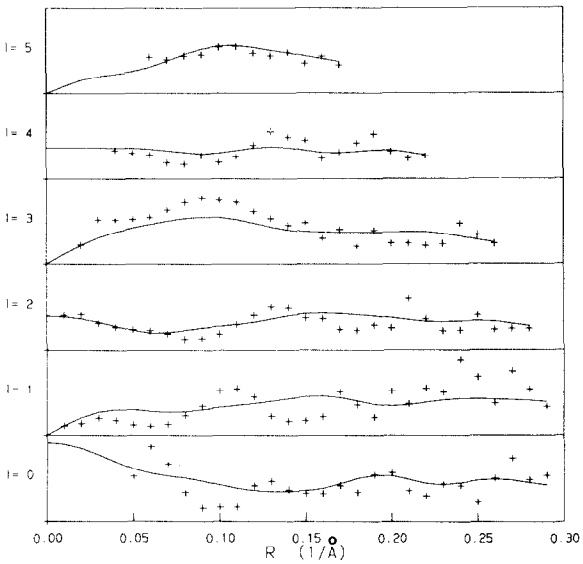

Fig. 2. Calculated amplitudes (———) of the cylindrically averaged Fourier transform of the best 2-fold helix (model 1) of CPS superimposed on the measured amplitudes (+) for layer lines 0–5. An isotropic temperature factor $B = 6$ Å^2 was applied to the calculated values.

TABLE III

Values of the major conformation angles (and estimated standard deviations) in the final model of CPS

Conformation angle	Values (°)
ϕ_1(O-5C–C-1C–O-4A–C-4A)	−85(2)
ψ_1(C-1C–O-4A–C-4A–C-5A)	−135(2)
χ_1(C-4A–C-5A–C-6A–O-6A)	−85(3)
ϕ_2(O-5A–C-1A–O-3B–C-3B)	67(2)
ψ_2(C-1A–O-3B–C-3B–C-4B)	101(4)
χ_2(C-4B–C-5B–C-6B–O-6B)	−172(3)
ϕ_3(O-5B–C-1B–O-3C–C-3C)	65(3)
ψ_3(C-1B–O-3C–C-3C–C-4C)	100(2)
χ_3(C-4C–C-5C–C-6C–O-6C)	70(7)
ϕ_4(C-2A–O-2A–C-1D–O-5D)	101(4)
ψ_4(C-1A–C-2A–O-2A–C-1D)	144(5)
χ_4(C-4D–C-5D–C-6D–O-6D)	−65(8)
ϕ_5(C-6A–O-6A–C-1E–O-5E)	−90(4)
ψ_5(C-5A–C-6A–O-6A–C-1E)	−100(4)
χ_5(C-4E–C-5E–C-6E–O-6E)	79(7)
ϕ_6(C-4E–O-4E–C-1F–O-5F)	−132(5)
ψ_6(C-3E–C-4E–O-4E–C-1F)	−127(4)
χ_6(C-4F–C-5F–C-6F–O-6F)	83(8)

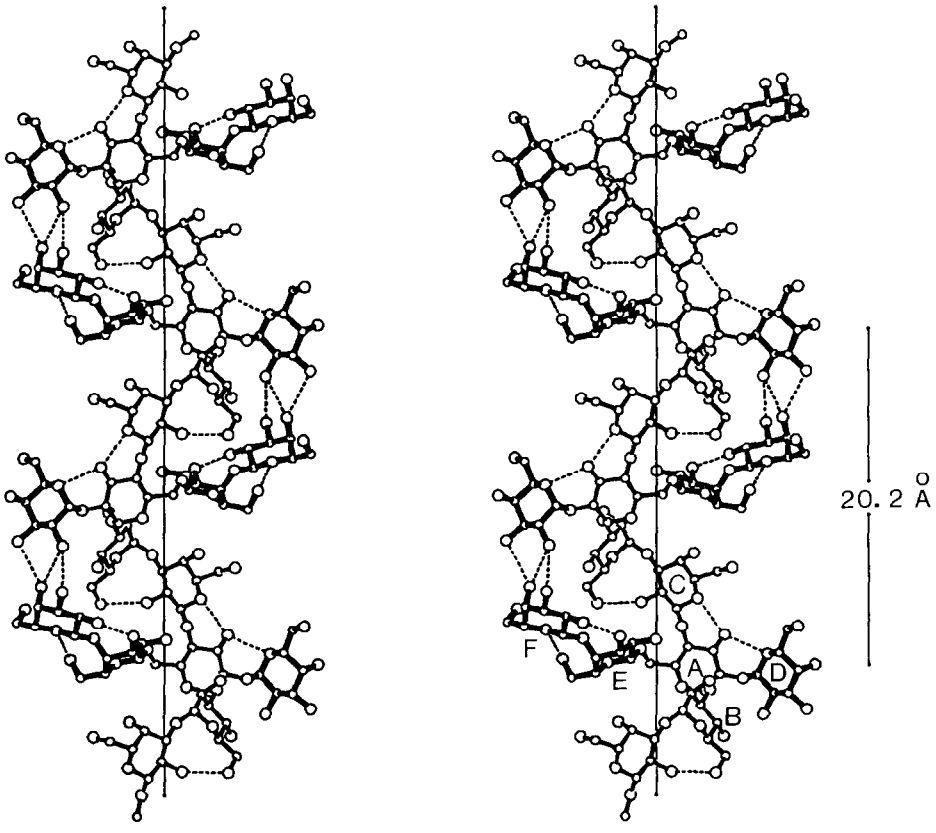

Fig. 3. A stereo view of two turns of the CPS 2-fold helix (model 1) normal to its helix axis (vertical line). With its side chains (▬) on the outside wrapping around the main chain (———), the molecule is stabilized by a network of hydrogen bonds (------) involving the side and main chains, and thus has the appearance of a "pseudo double helix".

TABLE IV

Intrachain hydrogen bonds that stabilize the CPS helix

Donor *X*	Acceptor *Y*	Precursor *P*	*X* ··· *Y* (Å)	*P*-*X* ··· *Y* (°)	Remarks
O-3A	O-5D	C-3A	2.79	103	bifurcated
O-3A	O-5C	C-3A	2.72	104	bifurcated
O-6B	O-2C	C-6B	3.00	93	
O-6E	O-5F	C-6E	2.80	105	
O-2F	O-3E	C-2F	2.52	116	
O-2D	O-3F	C-2D	3.03	147	
O-4F	O-2D	C-4F	3.03	122	bifurcated
O-4F	O-3D	C-4F	3.08	132	bifurcated

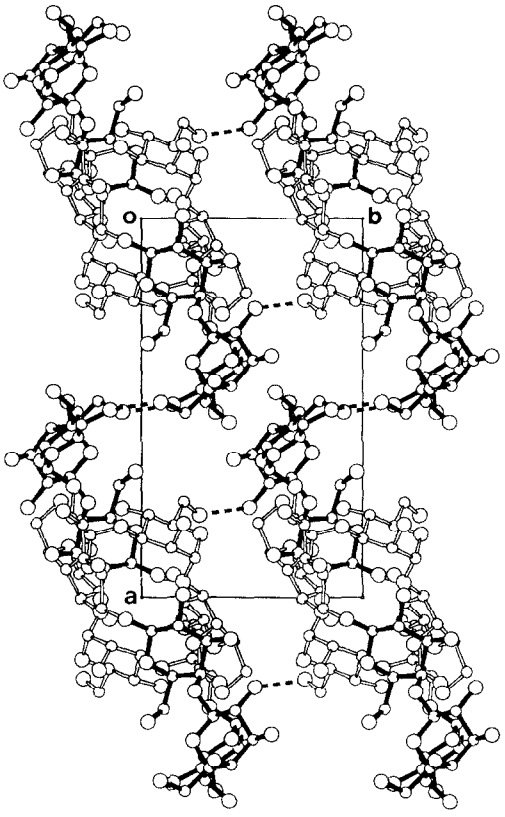

Fig. 4. A *c*-axis projection of the putative monoclinic unit cell, showing the parallel packing of the CPS molecules. Side chains (▬) are involved in the inter-chain hydrogen bonds (------) and are therefore necessary for the association of the molecules.

neighbors related by *a* and *b* translations as a function of μ, and later refining μ against these contacts as observations, the best value of μ was determined to be 53°. The resulting packing diagram viewed down the *c* axis (Fig. 4) illustrates how the molecules might interact in the crystalline state. Each molecule appears like an elongated rectangle, $\sim 19.6 \times \sim 9.0$ Å, the diagonal of which is approximately along a diagonal of the unit cell. Therefore, the crystalline arrangement may be thought of as parallel arrays of sheets of molecules with each sheet passing through this diagonal and the *c* axis. Molecules within a sheet display only van der Waals interactions. Between the sheets, however, the molecules form hydrogen bonds via the side chains. For example, along the *b* axis, the association is through O-6B · · · O-2F; along the *a* axis, it is through O-6D · · · O-6F. The former association is bifurcated, as O-6B is a donor in the previously mentioned intrachain hydrogen bond with O-2C (Table IV). In essence, each molecule is connected by interchain

hydrogen bonds to four out of six surrounding neighbors in this parallel packing arrangement.

The trigonal unit cell can accommodate two 2-fold single helices, e.g., one at the corner and one at the center, which may be positioned either parallel or antiparallel. Modeling analysis demonstrates that the best parallel arrangement occurs when both molecules have the same orientation and zero relative translation along the *c* direction. This setting reduces to that of the monoclinic unit cell described above. In the antiparallel arrangement, however, the two molecules may orient

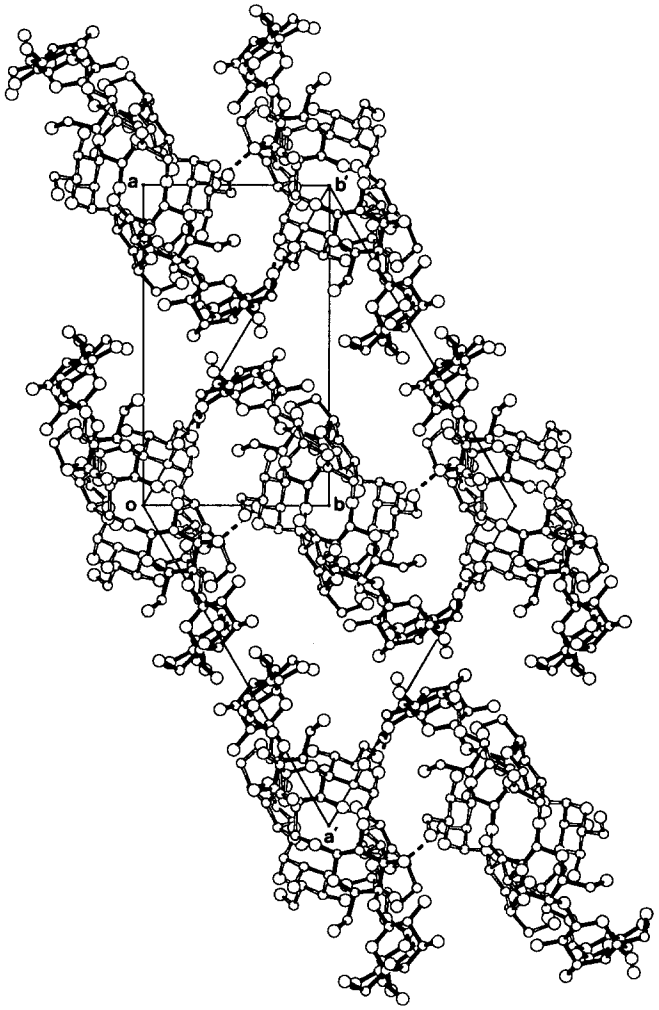

Fig. 5. A proposed model for the antiparallel packing arrangement of two CPS molecules in a trigonal unit cell viewed along the *c* axis. The side chain–side chain hydrogen bonds (------) show the importance of the side chains for the molecular aggregation and gelation.

differently and have non-zero relative translation along the *c* direction. The best packing arrangement[15] is shown in Fig. 5, which also illustrates the relationship between the monoclinic and trigonal unit cells. The molecule at the center is linked by hydrogen bonds (O-6D · · · O-5B and O-6D · · · O-2B, which are bifurcated, and O-3E · · · O-2B) to those of opposite polarity and this is accomplished by the side chains in the same way as in the parallel packing in the monoclinic unit cell. Thus, the results of the packing analysis stress the importance of the side chains for the association of the CPS molecules.

The trigonal cell is large enough to contain one half-staggered, parallel, double helix. However, for the models 6 and 9, which have reasonable X-ray fit, it is not possible to achieve any satisfactory packing because of severe steric compression between neighboring double helices. Therefore, these double-helical models were rejected from further consideration.

DISCUSSION

Normally, the presence of side chains on a polysaccharide backbone is considered to impede gelation. Examples are the three-branched polysaccharides welan, S-657, and rhamsan of the gellan family[4], and curdlan[19]-related schizophyllan[20]. The side chains of CPS, rather than inhibiting intermolecular association, appear to be essential both for the adoption of an ordered conformation of the molecule and for gel formation. The effect of chemical modification of the side chains on the solution properties of CPS has been investigated. Thus, after cleavage of the side chains by Smith degradation, the debranched polysaccharide remained as a disordered random coil at all temperatures and could not form gels in aqueous solution[6]. An ionic carboxylate derivative of the polysaccharide, prepared by partial oxidation with periodate and further oxidation with chlorite, failed[21] to form gels either by the addition of calcium ions or lowering the pH. Investigations of ionic and non-ionic derivatives of CPS also concluded[22] that gel stability was greatly diminished by chemical modifications of any kind. Enzymic removal of the monosaccharide side chains abolished hysteresis and gelation[23]. All these observations can be explained at the molecular level by the results now reported. The communication between the di- and mono-saccharide side chains of adjacent repeating units is the crucial step towards the formation of a robust "pseudo double helix" that has an ordered conformation. Furthermore, packing analysis has demonstrated that the interchain hydrogen bonds, which are responsible for intermolecular association, can be formed in CPS "pseudo double helices", mainly because of the side chains. Therefore, these side chains are important promoters of gel formation and it is suggested that, if the side chains are partly or fully removed, the remaining polysaccharide can neither retain any molecular order in solution nor promote gelation as efficiently as the native polysaccharide. The relevance of the "pseudo double helix" structure to conformational ordering and

intermolecular association under hydrated conditions is discussed further in an accompanying paper[23].

ACKNOWLEDGMENTS

This work was supported by research grants from the Purdue University Agricultural Experiment Station and the Purdue Research Foundation.

REFERENCES

1 R. Chandrasekaran, L.C. Puigjaner, K.L. Joyce, and S. Arnott, *Carbohydr. Res.*, 181 (1988) 23–40.
2 R.P. Millane, R. Chandrasekaran, S. Arnott, and I.C.M. Dea, *Carbohydr. Res.*, 182 (1988) 1–17.
3 R. Chandrasekaran, A. Radha, and V.G. Thailambal, *Carbohydr. Res.*, 224 (1992) 1–17.
4 E.J. Lee and R. Chandrasekaran, *Carbohydr. Res.*, 214 (1991) 11–24.
5 L.P.T.M. Zevenhuizen and A.R.W. Van Neerven, *Carbohydr. Res.*, 124 (1983) 166–171.
6 M.J. Gidley, I.C.M. Dea, G. Eggleston, and E.R. Morris, *Carbohydr. Res.*, 160 (1987) 381–396.
7 B. Lindberg, F. Lindh, J. Lonngren, and W. Nimmich, *Carbohydr. Res.*, 70 (1979) 135–144.
8 L.P.T.M. Zevenhuizen, *Appl. Microbial Biotechnol.*, 20 (1984) 393–399.
9 R. Chandrasekaran, R.P. Millane, J.K. Walker, S. Arnott, and I.C.M. Dea, in S.S. Stivala, V. Crescenzi, and I.C.M. Dea (Eds.), *Industrial Polysaccharides*, Gordon and Breach, New York, 1987, pp. 111–118.
10 R. Chandrasekaran, R.P. Millane, and S. Arnott, in G.O. Phillips, D.J. Wedlock, and P.A. Williams (Eds.), *Gums and Stabilizers for the Food Industry 4*, IRL Press, Oxford, 1987, pp. 183–191.
11 P.J.C. Smith and S. Arnott, *Acta Crystallogr., Sect. A*, 34 (1978) 3–11.
12 R.D.B. Fraser, T.P. MacRae, A. Miller, and R.J. Rowlands, *J. Appl. Crystallogr.*, 9 (1976) 81–94.
13 R.P. Millane and S. Arnott, *J. Appl. Crystallogr.*, 18 (1985) 419–423.
14 R.P. Millane and S. Arnott, *J. Macromol. Sci. Phys., Sect. B*, 24 (1985) 193–227.
15 R. Chandrasekaran, E.J. Lee, A. Radha, and V.G. Thailambal, in R. Chandrasekaran (Ed.), *Frontiers in Carbohydrate Research-2*, Elsevier, London, 1992, pp. 65–84.
16 S. Arnott and W.E. Scott, *J. Chem. Soc., Perkin Trans. 2*, (1972) 324–335.
17 W.C. Hamilton, *Acta Crystallogr.*, 18 (1965) 502–510.
18 D.A. Rees, I.W. Steele, and F.B. Williamson, *J. Polym. Sci., Part C*, (1969) 261–276.
19 T. Harada, A. Misaki, and H. Saito, *Arch. Biochem. Biophys.*, 124 (1968) 292–298.
20 T. Norisuye, T. Yanaki, and H. Fujita, *J. Polym. Sci. Phys. Ed.*, 18 (1980) 547–558.
21 A. Cesaro, S. Paoletti, F. Delben, S. Cavallo, V. Crescenzi, and L.P.T.M. Zevenhuizen, in S.S. Stivala, V. Crescenzi, and I.C.M. Dea (Eds.), *Industrial Polysaccharides*, Gordon and Breach, New York, 1987, pp. 99–109.
22 A. Cesaro, P. Esposito, C. Bertocchi, and V. Crescenzi, *Carbohydr. Res.*, 186 (1989) 141–155.
23 M.J. Gidley, G. Eggleston, and E.R. Morris, *Carbohydr. Res.*, 231 (1992) 185–196.